# Ruby as a Maser Material*

CHIHIRO KIKUCHI, JOHN LAMBE, GEORGE MAKHOV, AND ROBERT W. TERHUNE
*The University of Michigan, Willow Run Laboratories, Ann Arbor, Michigan*

(Received November 3, 1958)

The reasons for the initial choice of ruby as a maser material are outlined and some measurements of the parameters in the spin Hamiltonian and of spin relaxation times are reported. The relative merits of single- and double-pump modes of operation of a four-level maser are discussed and measurements of the oscillator power for the two cases are included.

## 1. INTRODUCTION

IN an earlier note[1] we reported briefly on some of the maser properties of ruby and indicated that such properties as chemical stability, thermal conductivity, and dielectric properties ultimately may determine the usefulness of ruby as a maser material. The purpose of the present paper is to describe our results in greater detail and to present new considerations which may be important to the design of a ruby maser. Many of the operational characteristics of a ruby maser will be presented in a later paper.

An extensive list of references on gaseous masers has been given in a paper by Townes and his students.[2] The suggestion of a solid-state maser using paramagnetic materials was made by Bloembergen,[3] who provided the basic theory, and proposed nickel fluosilicate and gadolinium ethyl sulfate as possible materials. The latter material was suggested independently by Scovil, who with his co-workers[4] at the Bell Telephone Laboratories demonstrated the feasibility of Bloembergen's proposal. Subsequently maser action in chrome cyanide was demonstrated by McWhorter and Meyer.[5] Paralleling these developments notable progress has been made in the areas of two-level masers and the microwave parametric amplifier. The two-level masers have been investigated by Feher[6] and his co-workers in silicon, and in neutron-irradiated quartz and MgO by Chester, Wagner, and Castle.[7] The parametric microwave amplifier was suggested by Suhl[8] and has been demonstrated subsequently by Weiss.[9] In our present paper, we are concerned only with the paramagnetic three- and four-level maser.

* This work was supported by Project Michigan under Department of the Army Contract, administered by the U. S. Army Signal Corps, and the Office of Scientific Research of the Air Research and Development Command.

[1] Makhov, Kikuchi, Lambe, and Terhune, Phys. Rev. **109**, 1399 (1958).

[2] Alsop, Giordmain, Townes, and Wang, Phys. Rev. **107**, 1450 (1957).

[3] N. Bloembergen, Phys. Rev. **104**, 324 (1956).

[4] Scovil, Feher, and Seidel, Phys. Rev. **105**, 762 (1957).

[5] A. L. McWhorter and J. W. Meyer, Phys. Rev. **109**, 312 (1958).

[6] Feher, Gordon, Buehler, Gere, and Thurmond, Phys. Rev. **109**, 221 (1958).

[7] Chester, Wagner, and Castle, Phys. Rev. **110**, 281 (1958).

[8] H. Suhl, Phys. Rev. **106**, 384 (1957); J. Appl. Phys. **28**, 1225 (1957).

[9] M. T. Weiss, Phys. Rev. **107**, 317 (1957).

## 2. SELECTION OF MATERIAL

When Bloembergen's suggestion of the solid-state maser became known, it was clear that the basic problem would be that of selecting a material in which conditions are most favorable for maser action. Since the reasoning that was employed may be useful in guiding the search for other materials for specific applications, the arguments which ultimately led to our selection of ruby for study will be indicated. To keep the effective number of spins high, the spin of the ground state for a three-level maser should be **1** or $\frac{3}{2}$. This meant that the paramagnetic ion should be $Ni^{++}$, $V^{++}$, or $Cr^{+++}$. Furthermore, since we were concerned primarily with the detection of maser action, the nuclear spin should preferably be zero, again in order to keep the effective number of spins high. Also, materials containing hydrogen should be avoided if possible, because in addition to the large nuclear moment which will adversely affect the spin-lattice relaxation time, the protons are generally present in the form of waters of hydration, which contribute to chemical instability and high dielectric losses. Furthermore, the crystalline lattice, which disperses the paramagnetic ions, should be as free of nuclear magnetic fields as possible. From this standpoint, a lattice such as that of ZnS would be satisfactory, if other conditions could be met. The zero-field splitting should be comparable to the signal frequency. This requirement stems from the fact that the admixing of spin states is most favorable when the Zeeman and the crystalline field terms are comparable. Of the chromium compounds measured, ruby[10–12] was known to have the second largest zero-field splitting, next only to chromium acetyl acetonate,[13] for which $\delta = 1.18$ cm$^{-1}$. The spin-lattice relaxation time of ruby was not known at the time, but it was felt that the relaxation time might be favorable because the chromium, occupying $Al^{+++}$ substitutional sites, would be surrounded by six oxygens, with aluminum as the second nearest neighbors. Also as our investigation progressed, it became clear that thermal conductivity might be an important factor.

[10] A. A. Manenkov and A. M. Prokhorov, Zhur. Eksptl. i Teoret. Fiz. **28**, 762 (1955) [translation: Soviet Phys. JETP **1**, 611 (1955)].

[11] M. M. Zaripov and Iu. Ia. Shamonin, Zhur. Eksptl. i Teoret. Fiz. **30**, 2911 (1956) [translation: Soviet Phys. JETP **3**, 171 (1956)].

[12] J. E. Geusic, Phys. Rev. **102**, 1252 (1956).

[13] L. S. Singer, J. Chem. Phys. **23**, 379 (1955).

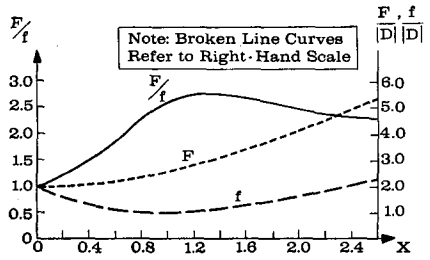


FIG. 1. Plot of $F(\mp\frac{3}{2}\leftrightarrow\pm\frac{1}{2})$, $f(\frac{1}{2}\leftrightarrow-\frac{1}{2})$ and their ratio as function of parameter $x$.

We would like to point out that $Ga_2O_3$:Cr, with optical properties similar to those of ruby, may fulfill some of the criteria enumerated in the foregoing.[14] Chromium in MgO appears attractive at first sight. According to Wertz and Auzins,[15] the zero-field splitting of $Cr^{+++}$ associated with a crystal defect in MgO is 0.082 $cm^{-1}$. However, the major fraction of the $Cr^{+++}$ ions are in a cubic crystalline field, and thus the ground state will not be split. This argument, however, does not preclude the feasibility of indirectly exciting the $Cr^{+++}$ ions in a cubic field, by means of those associated with defects. The possibility of indirect excitation has been shown recently by Shapiro, Bloembergen, and Artman.[16]

### 3. THEORY

It is generally assumed that in substituted sapphires, the paramagnetic impurities occupy sites of the metallic ions. The unit cell of $Al_2O_3$ contains two nonequivalent $Al^{+++}$ sites, but for paramagnetic ions of spin $\frac{3}{2}$ or less, as is the case of $Cr^{+++}$ ions, the two sites become magnetically equivalent. If, on the other hand, the spin is 2 or higher, such as that of $Fe^{+++}$ and $Mn^{++}$, for which $S=\frac{5}{2}$, the two sites become distinguishable. This effect was discovered experimentally in $CaCO_3$:Mn by Hurd, Sachs, and Hershberger,[17] and subsequently interpreted by Kikuchi[18] and McConnell.[19] The corresponding effect in $Al_2O_3$:Fe was reported recently by Kornienko and Prokhorov.[20]

Assuming then that all paramagnetic ions in the $Al_2O_3$ lattice are equivalent and independent, the appropriate spin-Hamiltonian is given by

$$\mathcal{H}=\beta S\cdot g\cdot H+D[S_z^2-(5/4)], \tag{3.1}$$

where $\beta$ is the Bohr magnetron; $S$ the electron spin operator with components $S_x$, $S_y$, and $S_z$; $H$ the magnetic field; $D$ the axial crystalline electric field, and $g$ the Zeeman $g$ tensor with components $g_{zz}=g_{\parallel}$, $g_{xx}=g_{yy}=g_{\perp}$. The preceding Hamiltonian leads to the eigenvalue equation

$$(\epsilon^2-1)^2-\tfrac{5}{2}x^2\epsilon^2+\tfrac{9}{16}x^4-x^2(5g_{\parallel}^2\cos^2\theta-g_{\perp}^2\sin^2\theta)/2g^2 +2\epsilon\lambda x^2(g_{\perp}^2\sin^2\theta-2g_{\parallel}^2\cos^2\theta)/g^2=0, \tag{3.2}$$

where

$$\epsilon=\frac{E}{|D|},\quad x=\frac{g\beta H}{|D|},\quad \lambda=\frac{D}{|D|},\quad g^2=g_{\parallel}^2\cos^2\theta+g_{\perp}^2\sin^2\theta.$$

If the crystal orientation is chosen so that

$$g_{\perp}^2\sin^2\theta=2g_{\parallel}^2\cos^2\theta, \tag{3.3}$$

the roots of the equation are given by

$$\epsilon(\pm\tfrac{3}{2})=\pm[1+(5/4)x^2+x(3+x^2)^{\frac{1}{2}}]^{\frac{1}{2}}, \tag{3.4}$$
$$\epsilon(\pm\tfrac{1}{2})=\pm[1+(5/4)x^2-x(3+x^2)^{\frac{1}{2}}]^{\frac{1}{2}}.$$

The resonance frequency causing transitions between electron spin states $M$ and $M'$ and will then be given by

$$hf_{MM'}=|D|\,|\epsilon(M)-\epsilon(M')|. \tag{3.5}$$

Consequently, the resonance frequencies for the transitions $-\frac{3}{2}\leftrightarrow\frac{1}{2}$ and $-\frac{1}{2}\leftrightarrow\frac{3}{2}$ are equal, given by

$$hF=|D|[\epsilon(\tfrac{3}{2})+\epsilon(\tfrac{1}{2})], \tag{3.6}$$

and that for the $-\frac{1}{2}\leftrightarrow\frac{1}{2}$ transition is

$$hf=2|D|\,\epsilon(\tfrac{1}{2}). \tag{3.7}$$

We note that the frequency ratio $F/f$ is a function of the parameter $x$ only. The ratio is plotted in Fig. 1. This plot of the magnetic field permits a determination of $|D|$ and $g$. The experimentally determined values of these quantities at room temperature and at 4.2°K are as follows:

| | 300°K | 4.2°K |
|---|---|---|
| $f$(kMc/sec) | 9.736 | 9.765 |
| $F$(kMc/sec) | 24.327 | 24.322 |
| $F/f$ | 2.4986 | 2.4908 |
| $H$(oersted) | 4216.3 | 4212.9 |
| $\|D\|$ ($cm^{-1}$) | 0.1937 | 0.1919 |
| $g$ | 1.97 | 1.98 |
| $\|D\|$ from zero field ($cm^{-1}$) | 0.1917 | 0.1909 |

The directly measured values obtained at zero magnetic field are given in the last row.

### 4. RUBY ISOFREQUENCIES

In designing a maser for a specific pumping or signal frequency, a convenient procedure is to plot a family of curves which give, at a given frequency, the dependence of a resonance absorption on the magnitude and orientation of the magnetic field. Such a plot is presented in Fig. 2. This particular plot can be used if the pumping frequency is fixed at 24 kMc/sec. If, on the other hand, the signal frequency is fixed, the family of curves for various pumping frequencies should be used.

The isofrequency curve for the transition $M\leftrightarrow M'$

[14] P. Pringsheim, *Fluorescence and Phosphorescence* (Interscience Publishers, Inc., New York, 1949), pp. 627.
[15] J. E. Wertz and P. Auzins, Phys. Rev. **106**, 484 (1957).
[16] Shapiro, Bloembergen, and Artman, Bull. Am. Phys. Soc. Ser. II, **3**, 317 (1958).
[17] Hurd, Sachs, and Hershberger, Phys. Rev. **93**, 373 (1954).
[18] C. Kikuchi, Phys. Rev. **100**, 1243 (1955).
[19] H. M. McConnell, J. Chem. Phys. **24**, 904 (1956).
[20] L. S. Kornienko and A. M. Prokhorov, Zhur. Eksptl. i Teoret. Fiz. **33**, 805 (1957) [translation: Soviet Phys. JETP **6**, 620 (1958)].

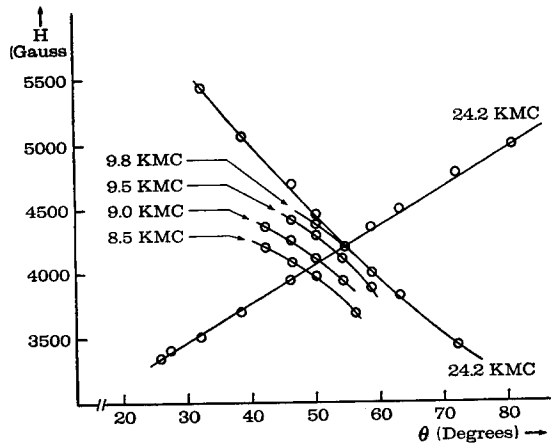


FIG. 2. Ruby isofrequencies.

satisfies the relation

$$d\epsilon(M)-d\epsilon(M')=0. \tag{4.1}$$

Differentiating the eigenvalue equation and putting $\cos^2\theta=\frac{1}{3}$ and $x=2$, we find

$$\begin{aligned} -\tfrac{1}{2}\leftrightarrow\tfrac{1}{2}&: \quad dx+1.27d\theta=0,\\ -\tfrac{3}{2}\leftrightarrow\tfrac{1}{2}&: \quad dx+(0.256+1.149\lambda)d\theta=0,\\ -\tfrac{1}{2}\leftrightarrow\tfrac{3}{2}&: \quad dx+(0.256-1.149\lambda)d\theta=0. \end{aligned} \tag{4.2}$$

Since $D$ is negative, $\lambda=-1$; so that the transition $-\frac{3}{2}\leftrightarrow\frac{1}{2}$ is the one with positive slope. The other two slopes are negative. The slopes are in the ratio $-1.18:(-1.57):1$. The ratio determined from the experimental plot is $-1.33:(-1.75):1$. These analyses indicate that the lower three levels are being used for amplification.

## 5. CAVITY DESIGN

To date several dual-resonance cavity designs, such as strip guide,[4,21] coaxial,[5] rectangular,[22] and re-entrant coaxial cavities,[23] have been used by different investigators. For our investigations a cylindrical cavity, designed to excite the $TE_{011}$ and $TE_{114}$ modes, was used for flexibility. The resonance frequencies of these modes are given by[24,25]

$$TE_{011}: \quad (fD)^2=c^2\left[\left(\frac{3.832}{\pi}\right)^2+\tfrac{1}{4}\left(\frac{D}{L}\right)^2\right] \tag{5.1}$$

and

$$TE_{114}: \quad (FD)^2=c^2\left[\left(\frac{0.841}{\pi}\right)^2+4\left(\frac{D}{L}\right)^2\right]. \tag{5.2}$$

The high-$Q$ $TE_{011}$ mode was used for the detection and amplification of the $X$-band signal. Since this frequency is associated with an "allowed" transition, the rf magnetic field at the center of cavity is always normal to the dc field as the magnet is swung on a vertical axis. For the $TE_{114}$ mode, the rf field is horizontal so that its angle with the dc magnetic field can be varied. This arrangement was used in our initial investigations because the angle of the rf field for optimum pumping was not known. Subsequent theoretical investigations indicated that considerable care is needed in designing a maser cavity. For example, for a three-level maser near 55°, it appears that the pumping efficiency does not depend critically upon the direction of the rf field as long as it is normal to the dc field.

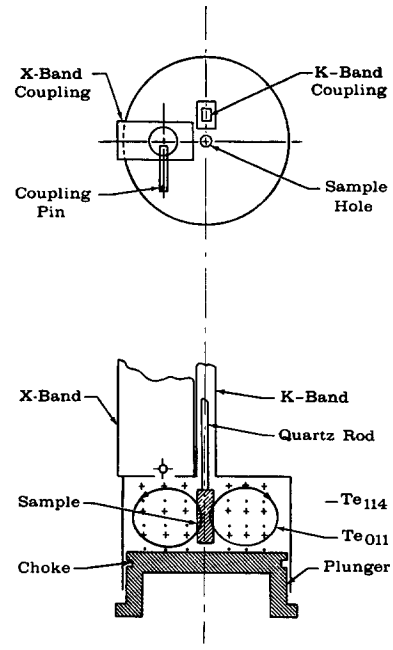


FIG. 3. Details of $K$- and $X$-band dual-mode cavity.

The magnetic field pattern and the coupling of the wave guide to the cavity are indicated in Fig. 3. The assembly to which the cavity is attached consists, in addition to stainless guides to provide thermal isolation, of mechanisms to tune and to vary the coupling of the cavity.

## 6. EXPERIMENTAL PROCEDURE AND RESULTS

The cavity assembly was installed in a double glass Dewar of about 1.5-liter capacity which permitted some six hours of continuous operation at 4.2°K. The crystal orientation was adjusted by means of sample holder and/or magnet on rotating mount, as needed. The pumping power was provided by a Varian VA-96 klystron, rated at 120 mw. All experiments were carried out at a fixed pumping frequency of 24.2 kMc/sec.

The $X$- and $K$-band systems consisted of conventional microwave and electronic equipment. A synchronous

[21] Artman, Bloembergen, and Shapiro, Phys. Rev. **109**, 1392 (1958).
[22] C. H. Townes (private communication).
[23] S. H. Autler and H. McAvoy, Phys. Rev. **110**, 280 (1958).
[24] *Techniques of Microwave Measurements*, MIT Radiation Laboratory Series, edited by C. G. Montgomery (McGraw-Hill Book Company, Inc., New York, 1947), Vol. II, p. 297.
[25] Wilson, Schramm, and Kinzer, Bell System Tech. J. **25**, 408 (1946).

detector[26] especially designed to provide flexibility was used when needed.

The initial, but unsuccessful, test to detect maser action in ruby was made on a dark synthetic ruby sample kindly loaned to us by J. E. Geusic. Subsequently maser action was observed on another synthetic ruby sample with nominal 0.1% $Cr_2O_3$ concentration, obtained from the Department of Mineralogy of The University of Michigan. The bulk of our measurements were made on a disk-shaped sample, about 10 grams in weight and $\frac{3}{4}$ in. in diam, cut from a boule of pink (0.1% $Cr_2O_3$) ruby purchased from Linde Air Products Company. The line width was found to be about 24 gauss, corresponding to $T_2^*=5\times10^{-9}$ sec, and almost independent of temperature.

The numerical value of the zero-field splitting was determined not only by the frequency-ratio method mentioned earlier, but also by measuring the resonance absorption frequency at zero magnetic field. The method was a modification of that used by Geusic. The sample was placed at the bottom of a wave guide located inside a Dewar. A magnetic field modulation was used to locate the point of zero-field resonance. The microwave power was derived from a Hewlett-Packard Model 686A sweep oscillator. At room temperature, resonance absorption occurred at 11.495 kMc/sec, corresponding to $\delta=0.3834$ cm$^{-1}$ and 11.445 kMc/sec at 4.2°K, or 0.3818 cm$^{-1}$. It is interesting to note that the nuclear quadrupole resonance splitting also decreases upon lowering the temperature. According to Spence[27] the splittings are 180.1 and 178.5 kc/sec at room and liquid helium temperatures, respectively, in the ratio of 1.009. The corresponding ratio of the zero-field splittings is 1.004.

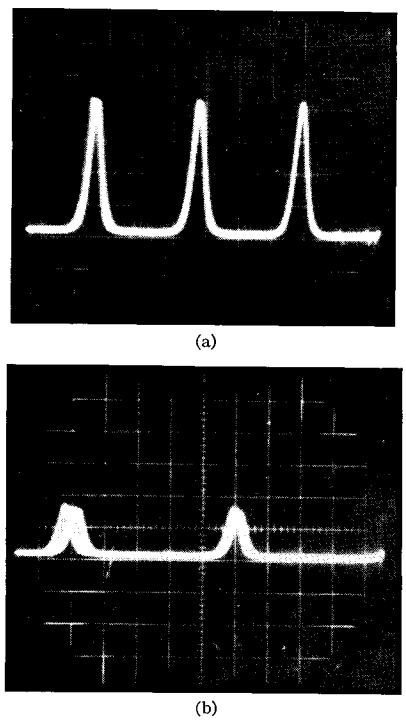

(a)

(b)

FIG. 4. Oscillation pulses. The pulses in (b) were obtained when the pump power was reduced. Note the decrease in pulse height and the increase in pulse interval.

[26] R. W. Terhune and J. Hickmott (unpublished).

The ruby maser was found capable of operating either as a pulse or a cw oscillator. By appropriate adjustment of the magnetic field and orientation, the cavity oscillation frequency was varied from 8.5 to 9.9 kMc/sec. The mode of operation as an oscillator was dependent on the amount of pumping power. At high levels of pumping, cw oscillations were obtained. A progressive decrease in $K$-band power first produced a ripple in the cw level, then discrete pulses. Pulse amplitude and repetition rate diminished with decreased pumping, as shown in Fig. 4. Figure 5 shows the dependence of pulse height and repetition rate upon pumping. The mechanism responsible for these oscillations is not known; however, it is tempting to assume that it is that of a relaxation oscillator.

Amplifying action in ruby was studied by sweeping the frequency of an $X$-band signal across the cavity resonance frequency. Figure 6 shows the observed effects. The lower trace was taken with the $K$-band power off; the upper trace was taken after turning on the $K$-band power. With appropriate adjustments, the ruby maser was tuned from about 8.5 to 9.9 kMc/sec. The gain band-width product realized with a sample containing about $10^{19}$ spins amounted to 40 Mc/sec. The spin-lattice relaxation time, measured by saturation and pulse techniques, yielded a value of about 25 msec.

Of particular significance is the ease with which the ruby maser operates at 4.2°K. The maser can also be operated with the liquid helium below the cavity level. A carbon resistor attached to the cavity indicated its temperature to be about 10°K. Since these results were obtained with the commercial pink ruby samples, a ruby maser operating at even higher temperature can perhaps be developed if specially prepared.†

## 7. SINGLE vs DOUBLE PUMPING

In the original three-level maser proposed by Bloembergen,[3] a serious limitation in the operation of the device may result from the "clogging" of the intermediate level, so that the pump frequency must be of the order of twice the signal frequency. In order to avoid these difficulties Scovil, Feher, and Seidel[4] doped gadolinium ethyl sulfate with $Ce^{+++}$ to decrease the spin-lattice relaxation time at the idler frequency. A similar procedure could be used for ruby by intentionally introducing paramagnetic crystal defects, chem-

[27] R. D. Spence (private communication).

† *Note added in proof.*—Several significant advances have been made while this paper was being processed. Maser action in ruby at 60°K was reported by C. R. Ditchfield and P. A. Forrester using push-pull pumping [Phys. Rev. Letters **1**, 448 (1958)], the traveling wave maser developed at the Bell Telephone Laboratories [DeGrasse, Schultz-DuBois, and Scovil, Solid State Circuits Conference, February 12–13 (1959)], and gain band width product in excess of 800 Mc/sec obtained by W. From [Microwave J. **2**, 9 (1959)].

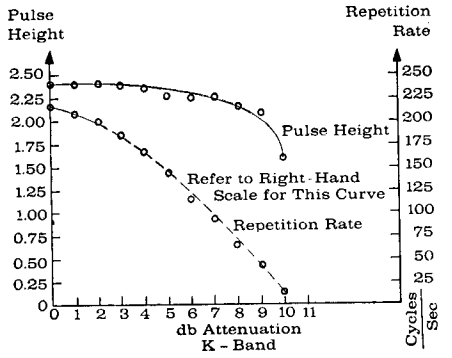


FIG. 5. Dependence of height and repetition rate of oscillation pulses from ruby.

ical or otherwise. A simple possible scheme would be to introduce color centers by gamma or neutron irradiation.

An alternative procedure particularly applicable to maser materials in which the paramagnetic ion has spin ($S=\frac{3}{2}$) is the double-pumping scheme. In the push-pull scheme, two pumps are used to populate and depopulate levels 2 and 3, respectively, between which the signal frequency is applied. The two pumps may be at two different frequencies, but a particularly interesting and also practical case arises when the two pumping frequencies are identical. This occurs when the energy levels are symmetrical, i.e., if

$$\cos\theta=\frac{g_\perp}{(2g_{||}^2+g_\perp^2)^{\frac{1}{2}}}\simeq\frac{1}{3^{\frac{1}{2}}},$$

since $g_\perp\simeq g_{||}$ for ruby.

The theory of the push-pull case can be easily developed by extending Bloembergen's analysis. The dynamical equations can be written in the form

$$\frac{dn_i}{dt}=\sum_{j=1}^{4}(n_j\alpha_{ji}-n_i\alpha_{ij}).$$

The coefficients $\alpha_{ij}$ include both the relaxation and radiation terms. For example, for single pumping between levels 1 and 3, the signal between 2 and 3,

$$\alpha_{13}=\omega_{13}+P_{13},\quad \alpha_{31}=\omega_{31}+P_{13},$$
$$\alpha_{23}=\omega_{23}+S_{23},\quad \alpha_{32}=\omega_{32}+S_{23},$$

and for all others, $\alpha_{ij}=\omega_{ij}$. The $\omega_{ij}$'s are the transition probabilities, as in Bloembergen's paper,[3] and the notations $P_{ij}$ and $S_{ij}$ have been introduced to designate pump and signal respectively. The results are as follows:

A. Single pump: $P_{13}$, $S_{32}$.

$$n_3-n_2=\frac{Nh}{4kT}\times\frac{\omega_{42}(\omega_{41}\nu_{21}-\omega_{43}\nu_{32})+(\omega_{41}+\omega_{42}+\omega_{43})(\omega_{21}\nu_{21}-\omega_{32}\nu_{32})}{\omega_{42}(\omega_{41}+\omega_{43})+(\omega_{41}+\omega_{42}+\omega_{43})(\omega_{21}+\omega_{32}+S_{32})}.$$

B. Single pump: $P_{24}$, $S_{32}$.

$$n_3-n_2=\frac{Nh}{4kT}\times\frac{\omega_{31}(\omega_{21}\nu_{32}-\omega_{41}\nu_{43})+(\omega_{12}+\omega_{13}+\omega_{14})(\omega_{32}\nu_{32}-\omega_{43}\nu_{43})}{\omega_{31}(\omega_{21}+\omega_{41})+(\omega_{12}+\omega_{13}+\omega_{14})(\omega_{23}+\omega_{34}+S_{23})}.$$

C. Double pump: $P_{13}$, $P_{24}$, $S_{32}$.

$$n_3-n_2=\frac{Nh}{4kT}\,\frac{\omega_{41}\nu_{41}+\omega_{43}\nu_{43}+\omega_{21}\nu_{21}-\omega_{32}\nu_{32}}{\omega_{12}+\omega_{23}+\omega_{14}+\omega_{23}+S_{32}}.$$

Other combinations of pumps and signal can be developed. In the first two cases the expression for the population difference reduces to that of Bloembergen if the terms involving levels 4 and 1 are omitted in cases A and B, respectively. For case C there are two limiting cases of interest: if $\omega_{41}\sim\omega_{32}$, the pump and the signal frequencies can be comparable; on the other hand, if $\omega_{41}=0$, $f$ (pump)$\sim 3f$ (signal)/2. In any case a more favorable pump-to-signal frequency ratio is possible, with corresponding improvement in maser performance. For one setting, the oscillator power increased by a factor of 4 when set at the push-pull angle.

It should be noted that push-pull operation is possible even for crystals having nonvanishing rhombic field. For the spin-Hamiltonian

$$\mathcal{H}=g\beta S\cdot H+D[S_z^2-(5/4)]+\tfrac{1}{2}E(S_+^2+S_-^2),$$

where $E$ is the rhombic crystalline field, the eigenvalue equation is

$$\begin{aligned}\lambda^4&-2\lambda^2[D^2+3E^2+(5/4)g^2\beta^2H^2]\\&+\lambda g^2\beta^2[2D(H_+H_--2H_z^2)-3E(H_+^2+H_-^2)]\\&+D^4+\tfrac{9}{16}g^4\beta^4H^4+\tfrac{1}{2}g^2\beta^2D^2(H_+H_--5H_z^2)+9E^4\\&+6E^2D^2+(9/2)g^2\beta^2E^2(H_z^2-H_+H_-)\\&+3g^2\beta^2(H_+^2+H_-^2)DE=0,\end{aligned}$$

so that the equation is factorable if

$$2D(H_+H_--2H_z^2)=3E(H_+^2+H_-^2).$$

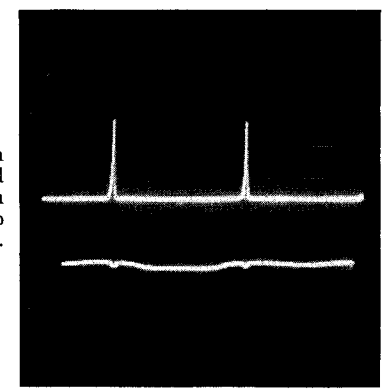

FIG. 6. Maser action of ruby. The lower and upper traces were taken with the $K$-band pump off and on, respectively.

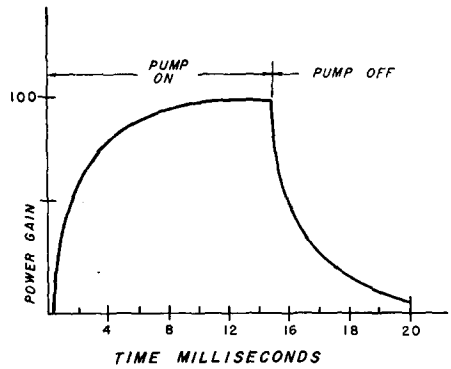


FIG. 7. Plot of time dependence of power gain.

This leads to

$$\cos^2\theta=\frac{D-3E\cos 2\phi}{3(D-E\cos 2\phi)}.$$

The energy levels are now given by

$$\lambda=\pm\{1+3r^2+(5/4)x^2 \pm x[x^2+9\cos^2\theta+3r^2x^2(4-3\cos^2\theta)]^{\frac{1}{2}}\}^{\frac{1}{2}},$$

instead of by Eq. (3.4). Here $r=E/|D|$.

### 8. GAIN DECAY AND SPIN-LATTICE RELAXATION TIME

One of the important properties of a maser material is of course the spin-lattice relaxation time. This is also of special interest here since it has recently been proposed that the usual methods of measurements of spin-lattice relaxation time may not give a correct picture of the relaxation which actually occurs when an inverted spin is produced.[2] The essential point is that the lattice may be the "bottleneck" in the flow of energy from the relaxing spin system to the temperature bath. This will have the effect of producing a pseudo-spin-lattice relaxation which can be much longer than actual spin-lattice relaxation time. This pseudo-spin-lattice relaxation time is what one would measure in normal saturation experiments. When an inversion is produced, however, the relaxation will display the true spin-lattice relaxation.

In the present work we have carried out pulse-type relaxation experiments to explore the above considerations. With ruby operating as a three-level maser, the pump power (level 1 to 3) was pulsed on and off, and maser action was used to explore the population decay between levels 2 and 3. In addition, with no pump power applied, a large saturating signal was applied between levels 2 and 3 and the decay observed. The experiments were carried out by applying square wave modulation to "Gyraline" ferrite modulators.

In the first type of experiment sufficient pump power was applied in the on-time to produce substantial gain. This gain was observed by applying an $X$-band test pulse to the cavity at random times. By taking a time exposure a complete picture of the decay is obtained as shown schematically in Fig. 7. The gain-decay time is seen to be of the order of a millisecond.

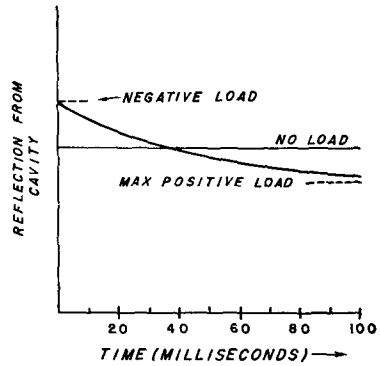


FIG. 8. Plot of population decay.

In the next case, the pump power is reduced so that only a slight inversion of population is produced. In this case a random $X$-band signal is swept across the cavity and the energy reflected from the cavity is observed. The cavity is undercoupled at zero field for this study. As the spin population relaxes to its normal distribution the magnetic load in the cavity varies from negative (inverted) to positive. The behavior of the cavity was observed through this transition to see if any significant changes occurred.

In Fig. 8 is shown the result of this measurement. There is a smooth decay from inversion through equal population to normal Boltzmann distribution. The decay time is 30 msec.

For the third case no $K$-band pump is used. Here the $X$-band signal was pulsed from a large saturating value to a low level. The recovery from saturation was then observed. Decay times of 20 to 30 msec were observed.

In order to relate the preceding measurements, the relationship between gain decay and population decay must be deduced.

The spin-lattice relaxation can be readily deduced from

$$G=[(1-\beta)/(1+\beta)]^2,$$

which relates the maser gain to the voltage standing wave ratio. Under matched conditions at zero-field the preceding expression reduces to

$$G^{\frac{1}{2}}=Q_0/(2|Q_m|-Q_0),$$

where $Q_m$ is the quality factor associated with magnetic losses or gain, and $Q_0$ is the unloaded quality factor in the absence of a magnetic field. It follows then that

$$\frac{1}{|Q_m|}=\frac{2G^{\frac{1}{2}}}{Q_0[1+G^{\frac{1}{2}}]}.$$

Since the reciprocal of the magnetic quality factor is proportional to the population difference $n_3-n_2$, the plot of the preceding expression gives the spin-lattice relaxation time. Measurements yield a decay time of about 25 msec. Of further interest is the approximate equality of the spin-decay time for positive and negative

spin temperatures. This seems to indicate that the phonon distribution is not appreciably different from the thermal equilibrium value. The reason for this may be the exceptionally high thermal conductivity of sapphire and ruby.[28]

### 9. DISCUSSION

Experience at this laboratory indicates that pink ruby is a good maser material from several standpoints. All Linde pink ruby samples, rated at 0.1% chromium concentration, have yielded satisfactory results. It was noticed that samples prepared from some of the boules showed a multiplicity of absorption lines, probably due to some type of crystalline imperfection: this, however, does not appear to affect the maser performance. The ease of operation should also be emphasized. This stems from the fact that the chromium ions in the two $Al^{+++}$ substitutional sites are magnetically equivalent and also from the fact that the rhombic field is zero. The excellent thermomechanical properties should be noted. Samples can be prepared easily and can withstand repeated thermal shocks. Also the gain band width is high. Recently Morris, Kyhl, and Strandberg[29] have reported a gain band width product of 43 Mc/sec.

### ACKNOWLEDGMENTS

We are indebted to R. Ager, M. Bair, A. Birko, L. Cross, J. Cook, and J. King for technical assistance.

[28] Berman, Foster, and Rosenberg, *Report on the Conference on Defects in Crystalline Solids* (The Physical Society, London, 1955).

[29] Morris, Kyhl, and Strandberg, Proc. Inst. Radio Engrs. (to be published).

JOURNAL OF APPLIED PHYSICS VOLUME 30, NUMBER 7 JULY, 1959

# Synthesis of a (110) [001] Type Torque Curve in Silicon Iron

C. G. DUNN AND J. L. WALTER
*General Electric Research Laboratory, Schenectady, New York*

(Received November 17, 1958)

The orientations and sizes of all the grains in a polycrystalline disk specimen of high-purity 3.25% silicon iron are measured to determine a calculated magnetic torque curve and the texture of the specimen. The torque results agree with the experimentally determined values. The curves approximate a (110) [001] single crystal torque curve, which is reduced about 75%, and thus indicate a possible texture consisting of about 25% (110) [001] and 75% random. The true texture obtained from the orientation data is found to have more than ten components, none of which is (110) [001]. Illustrations showing how a (110) [001] type torque curve may be synthesized from non-(110) [001] type components in the texture are given.

DESPITE known limitations to the determination of textures from magnetic torque curves extensive and useful measurements have been made for this purpose.[1–5] For the case of a relatively strong texture, such as (110) [001] in silicon iron, the torque method has been invaluable; but for weak or complex textures this method is unreliable. An example illustrating this point was encountered recently during the course of a study of textures in high-purity silicon iron. The present paper gives some results of a quantitative nature.

Particular importance is attached to the (110) [001] type torque curve. In the analytical method of Akulov and Bruchatov[1] a (110) [001] texture component takes a prominent position in the analysis of the torque curve. Also the primary recrystallization material, or matrix for growth of (110) [001] oriented grains during secondary recrystallization in silicon iron, produces a torque curve of the (110) [001] type.[6,7] Unfortunately the texture of this particular matrix has not been determined accurately enough by the pole figure method to account for the observed torque.[8–10] Also, the grains generally are not large enough in this material to x-ray conveniently for an orientation analysis grain-by-grain.

In the present investigation the grains were large enough for a grain-by-grain analysis. The orientation data obtained in this way were conveniently summarized with the aid of axis density figures. Also it was possible to calculate the torque contribution of every grain in a polycrystalline disk specimen and thus to consider the net torque as a synthesis of various types of torque curves. The result is compared with the experimentally determined torque curve.

### VARIATION OF TORQUE WITH CRYSTAL ORIENTATION

Tarasov and Bitter[11] have derived an equation giving the torque of a single crystal disk in terms of the orientation of the crystal and the first anisotropy constant $K_1$. Three angles, which are defined by the

[1] N. Akulov and N. Bruchatov, Ann. Physik **15**, 741 (1932).
[2] N. P. Goss, Trans. Am. Soc. Metals **23**, 511 (1935).
[3] L. P. Tarasov, Trans. Am. Inst. Mining Met. Engrs. **135**, 353 (1939).
[4] F. Bitter, *Introduction to Ferromagnetism* (McGraw-Hill Book Company, Inc., New York, 1937).
[5] L. R. Blake, Brit. J. Appl. Phys. **5**, 99 (1954).
[6] H. C. Fiedler, J. Appl. Phys. **29**, 361 (1958).
[7] C. G. Dunn, J. Appl. Phys. **30**, 850 (1959).
[8] C. G. Dunn, J. Appl. Phys. **29**, 1608 (1958).
[9] J. R. Brown, J. Appl. Phys. **29**, 359 (1958).
[10] P. K. Koh and C. G. Dunn (to be published).
[11] L. P. Tarasov and F. Bitter, Phys. Rev. **52**, 352 (1937).